Available online at www.sciencedirect.com
ScienceDirect
Journal of Photochemistry and Photobiology A: Chemistry 183 (2006) 133–137
Journal of Photochemistry and Photobiology A:Chemistry
www.elsevier.com/locate/jphotochem

Glass frit overcoated silver grid lines for nano-crystalline dye sensitized solar cells

Won Jae Lee [a,*], Easwaramoorthi Ramasamy [a,b], Dong Yoon Lee [a], Jae Sung Song [a]

[a] *Electric and Magnetic Devices Research Group, Korea Electrotechnology Research Institute, P.O. Box 20, Changwon 641-120, South Korea*
[b] *University of Science & Technology, Daejeon 305-333, South Korea*

Received 6 October 2005; received in revised form 5 January 2006; accepted 3 March 2006
Available online 18 April 2006

Abstract

Nano-crystalline dye sensitized solar cells (nc-DSSC) are promising alternative to expensive conventional solar cells. Relatively low efficiency in large size cell is also one of the factors that delayed the entry of this type cells in commercial market. Performance of large size DSSCs is always poor than small size cells because of high resistive losses associated with transparent conductive glass substrate. Here we show a simple method to reduce resistive loss, also, efficient collection of photogenerated carriers through silver grids which are prepared on both working electrode and counter electrode substrates by screen printing method in analogy to conventional silicon solar cells. For long-term stability, to protect corrosion of silver grids in electrolyte environment and to avoid charge recombination between silver grids and electrolyte, silver grids were overcoated by glass frit layer. Under simulated light (air mass 1.5, P_{in} 1000 W/m^2), glass frit overcoated silver grid cell shows 4.68% over all light to energy conversion efficiency.

Keywords: Silver grid; Redox electrolyte; Resistive loss; Overcoat layer

1. Introduction

Nano-crystalline dye sensitized solar cells (nc-DSSCs) have attracted an increasing number of academic and industrial researchers because of its high energy conversion efficiency and potentially low production cost. Since Grätzel's breakthrough report in Nature [1], high commercial expectations have been placed on DSSCs. Industrial researchers put their effort to scaling up the DSSC technology from laboratory level to practical applications such as stand-alone power generators, functional windows. In general, scaling up of DSSC technology falls in two categories; series monolithic or interconnect modules and parallel grid modules. Monolithic modules are formed by connecting small stripe cells in serious. Here each unit cell is prepared in ideal condition, so one can expect high performance as same as small size cell. On the other hand, parallel grid modules are prepared on single large size conductive glass substrates (usually 10 cm × 10 cm) with metal grids to reduce the resistive losses.

Each module has its own merits related to its application. In the case of transparent window applications [3], parallel grid modules have more advantage than monolithic with respect to active area (area used to generate electricity/total area) and low cost associated with simple production methods [4,5]. If large size, parallel grid cells are prepared by using the laboratory level technology and materials, overall light to energy conversion efficiency is very low because of high sheet resistance of large size transparent conducting glass substrates, leading to low fill factor [2]. In order to decrease sheet resistance of the conductive glass substrate and to collect photo-excited carriers more effectively; metal current collectors are prepared on conducting glass surface in analogy with conventional photovoltaic cells.

Silver is metal of choice because of its low electrical resistance and dark current. However, if we use silver grid lines in DSSCs, it should be protected from highly active redox electrolyte by chemically stable insulating overcoat layer; otherwise it will be corroded by I^-/I_3^- redox electrolyte. Also direct con-

* Corresponding author. Tel.: +82 55 280 1643; fax: +82 55 280 1590.
E-mail address: wjlee@keri.re.kr (W.J. Lee).

1010-6030/$ – see front matter © 2006 Elsevier B.V. All rights reserved.
doi:10.1016/j.jphotochem.2006.03.006

tact between silver grids and electrolyte leads to increase dark current through charge recombination. Some groups were protected the silver grids from redox electrolyte by surlyn sheet lamination [6,7], glass ceramic overcoat layer [8] while others applied anti-corrosion coating on silver grids [9]. Okada et al. studied feasibility of nickel as a candidate for grid line application because of its high stability against I^-/I_3^- redox electrolyte [2,10]. These methods are still not suitable for roll to roll manufacturing process because of their complicated mechanism. In this respect, here we show a simple industrial method to protect silver grids by applying glass frit overcoat layers on silver grids. Silver current collectors and insulating overcoat layers were formed on transparent conducting glass substrate by screen printing. Using these substrates, devices are prepared and their *I–V* characteristics have studied for range of light intensities and compared with normal devices, which do not have Ag grids.

2. Experiment

2.1. Silver metal grids

Silver is a metal of choice for grid line application in solar cells because of its high conductivity and low dark current. Also making screen printable silver paste with high conductivity is easy. Silver grid lines (dimension, length × width × height: 45 mm × 0.5 mm × 20 μm) were printed on conductive glass substrate (Solaronix FTO, 75% transmittance in visible range, R_s 10 Ω/□) using screen printable silver paste (Sung Jee Tech Co., Korea) by semi-automatic screen printing (Automax). After dried at 180 °C for 10 min, insulating glass frit (Sung Jee Tech Co., Korea) layer (dimension, length × width × height: 40 mm × 2 mm × 40 μm) was overcoated on silver grid line surface by specially designed screen that cover the whole surface of the metal grids except bus bar and then cured at 180 °C for 10 min. Two point measurement shows resistance of the 5 cm length, glass frit overcoated silver grid line is around 1 Ω.

2.2. TiO_2 working electrode

TiO_2 colloidal paste is prepared by mixing of 1 g hydroxyl benzoic acid (Aldrich) with 80 g anhydrous ethanol (Aldrich) and 60 g of TiO_2 powder (Deagussa, P25) followed by sonic mixing. This mixture is kept in high energy ball milling (150 rpm) for 30 min. Removing the ethanol from this mixture by the help of decicator attached with rotary pump leads to white compact powder. Forty grams of this powder is slowly mixed with mixture of 35 g of 95% terpinol and 5% ethyl cellulose. After getting the homogeneous, high viscous paste; 50 g of terpinol was added and mixed thoroughly by kneader. This paste kept in three roll ball milling for 10 min for homogeneous mixing. A screen with 20 μm thick, 200 mesh/in. is used to obtain approximately 10 μm thick TiO_2 layer. This layer is kept in room temperature for 15 min for drying and then sintered at 450 °C for 30 min. After cooling down to 80 °C, sintered TiO_2 layers were immersed in 0.15 mM dye solution (*cis*-bis(isothiocyanato)bis(2,2′-bipyridyl-4,4′-dicarboxylato) ruthenium(II) in ethanol, generally known as N3) for 24 h. Excess dyes are removed by rinsing the electrodes in anhydrous ethanol.

2.3. Counter electrode and device preparation

Thin layer of platinum was deposited on FTO glass substrates by means of electro deposition method (H_2PtCl_4 in DI water, $T_d \sim 60$ s, $J \sim 5$ mA/cm^2). In order to prepare sandwich type cell, counter electrode is directly placed on top of the sensitized TiO_2 layer, in between them surlyn polymer sheet (thickness ∼40 μm) was kept as a spacer for avoid direct contact between TiO_2 surface and counter electrode. Using hot press cell is sealed. The electrolyte contains I^-/I_3^- redox couple in acetonitrile solvent was introduced into the cell through predrilled holes in counter electrode side, then, holes are sealed using Amosil.

2.4. Device characterization

I–V characteristics of the DSSCs were measured using Keithley digital source meter (Model 2400) in both dark and illuminated condition. Solar simulator (Oriel) attached with 300 W Xenon lamp was used as light source. The desired light intensity was achieved by adjusting the lamp voltage. Optical microscope (Nikon) was used to record the vertical view for the glass frit overcoated Ag metal grids. Scanning electron microscope (Hitachi S4800) was employed to record cross-section view of metal grids. Alpha tencor step profiler meter was used to measure the thickness of the metal grids and overcoat layers. In order to study the effect of silver lines over DSSC performance, devices are prepared with same parameters without silver grids. Also to compare the performance of glass frit overcoated Ag grid DSSCs, surlyn sheet laminated Ag grid DSSC prepared by as mentioned in reference [6].

In this study, all cells have same dimension (length: 35 mm; width: 4 mm) and an active area equivalent to 1.4 cm^2. The distance between TiO_2 layer and silver current collector is fixed to 2 mm. Fig. 1 shows the photographs of the DSSCs with glass frit overcoated Ag grids (a) and surlyn sheet laminated Ag grids (b).

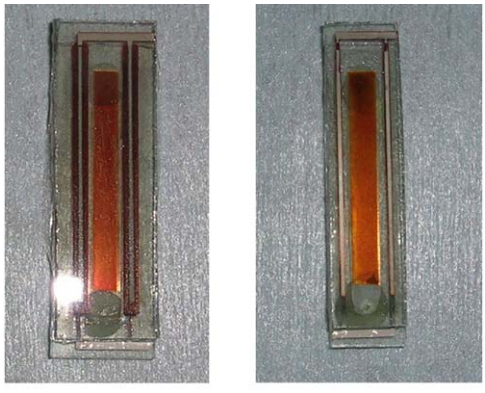

(a) (b)

Fig. 1. DSSCs with silver grid lines. (a) Glass frit overcoated Ag grids and (b) surlyn sheet laminated Ag grids.

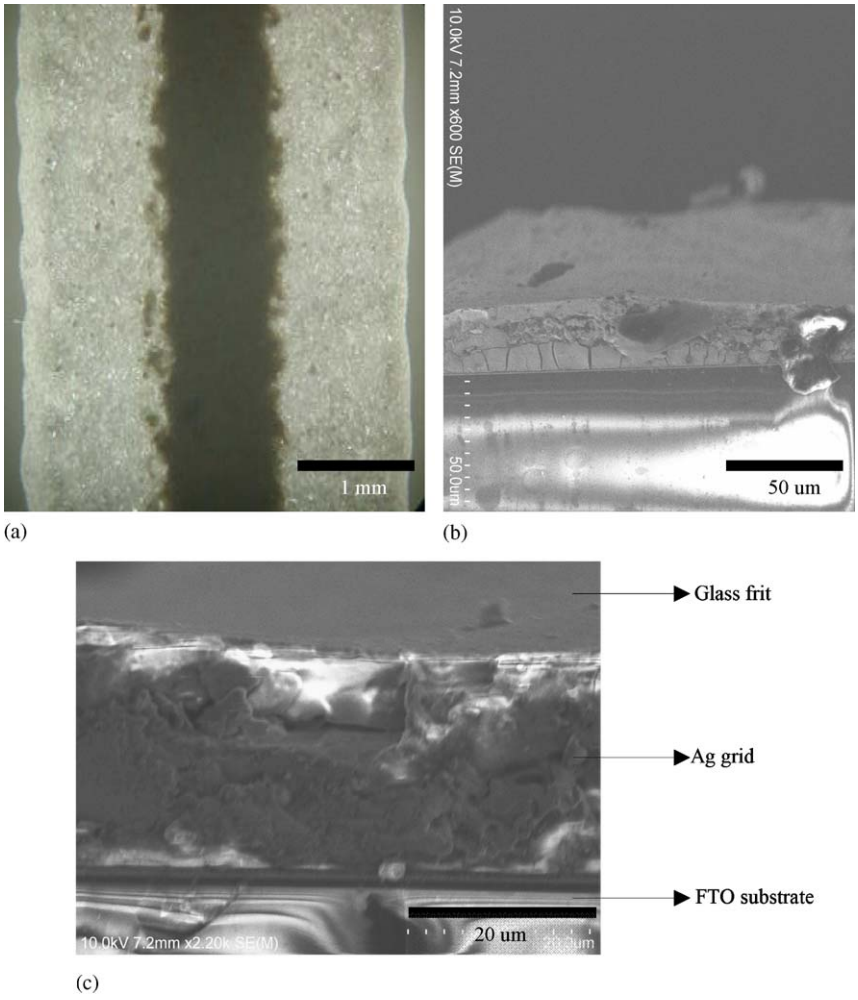

Fig. 2. SEM images of glass frit overcoated silver lines on FTO glass substrate (after sintering at 450 °C for 30 min), in (b and c) bottom layer: FTO glass, middle layer: Ag grid line and top layer: glass frit. (a) Top view, (b) cross-section view and (c) high resolution cross-section view.

3. Results and discussion

3.1. Microstructural characterization

Microstructural characterization of glass frit overcoated Ag grids revealed the formation of pinhole and crack free overcoat layer on silver grid lines. Fig. 2a shows top view of crack free glass frit overcoated silver line. From the cross-section view (Fig. 2b) one can see few vertical cracks that were originated from sintering at 450 °C for 30 min. These vertical cracks in Ag grid lines did not affect the conductivity because silver lines are ~500 μm wide. Even sintering at 450 °C not leads to any cracks in glass frit layer because of its lower thermal expansion coefficient. FTO/Ag and Ag/glass frit interfaces are clearly seen from magnified cross-section view (Fig. 2c). Good adherence between Ag lines and FTO surface leads to ohmic contact nature

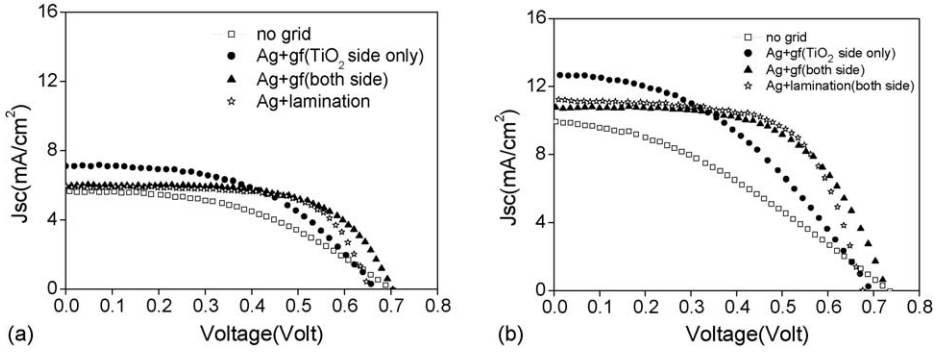

Fig. 3. *I–V* curve of stripe type DSSCs. Light intensity: (a) 60 mW/cm^2 and (b) 100 mW/cm^2.

and efficient photogenerated carrier collection. An alpha step measurement shows that each layer (silver/glass frit) has 20 μm thick. SEM measurement also confirms this value.

3.2. Photocurrent–voltage measurements

The slope of the *I–V* curve after maximum power point directly related to the series resistance of the cell. In DSSC, series resistance is composed of R_{TCO} (sheet resistance of FTO glass substrate) and charge transfer resistance (R_{CT}) of FTO/TiO_2 interface. Here decrease in slope means decrease in R_{TCO} because R_{CT} is fixed in all cases.

Fig. 3 shows the photocurrent–voltage curve of the stripe type DSSCs measured under two different light intensities. The cells prepared from glass frit overcoated silver grid FTO glass substrates have higher fill factor than normal devices which do not have silver grids. Particularly in standard conditions (air mass (AM) 1.5, P_{in} 1000 W/m^2), the losses associated with R_{TCO} are apparent. Even though current density maintains the linear relationship with incident light intensity, drop in fill factor leads to low overall light to energy conversion efficiency. DSSCs having silver grids on both sides (TiO_2 side and counter electrode side) maintain its fill factor almost constant for range of light intensities. For comparison, same size cells with surlyn polymer sheet laminated Ag grid are also prepared by following reference [6]. Due to thick, overcoated Ag grids on both sides; inter-electrode distance (gap between two electrodes) is 80 μm. In this case, I^-/I_3^- redox couples will migrate more distance than in the case cells with laminated Ag grids. So glass frit overcoated cells are expected to have less short circuit current than laminated one. Increase in shunt resistance in the former one suppressing the dark current and leads higher open circuit voltage.

Fig. 4 shows current density and fill factor of three different cells as s function of light intensity. At low intensity illumination, all cells have same short circuit current density. Exponential relation between current and resistance leads lower fill factor, especially under one sun condition in cells without current collector while cells with Ag grids showing small decline in fill factor. The performance of the glass frit overcoated Ag grid cell is comparable with surlyn laminated Ag grid cell.

3.3. Dark current

Fig. 5 shows the current–voltage curve of the DSSCs under dark conditions. Recombination of charge carriers by reduction of I_3^- at dye free TiO_2 surface or bare FTO surface exposed to

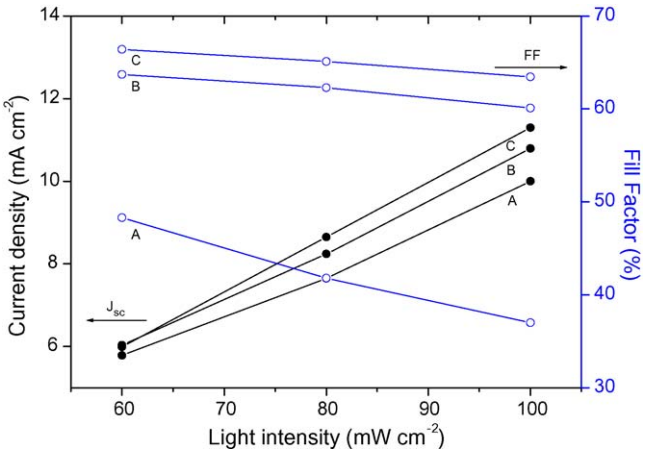

Fig. 4. J_{sc} and fill factor as a function of light intensity: (A) cells without Ag grids, (B) cells with glass frit overcoated Ag grids (spacer thickness 80 μm) and (C) cells with surlyn sheet laminated Ag grids. Closed circle: short circuit current density; open circle: fill factor.

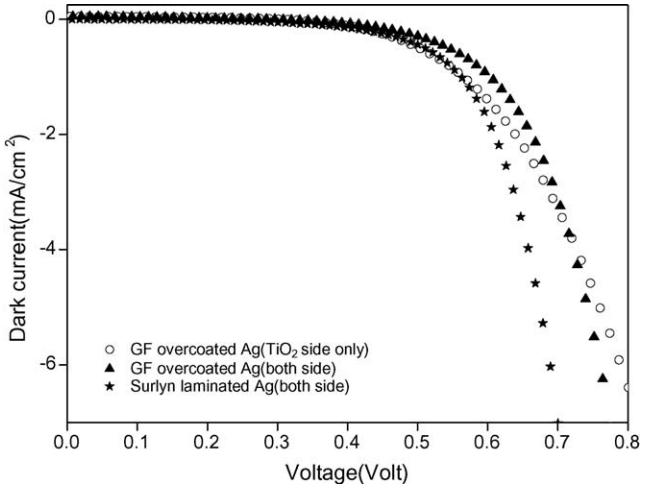

Fig. 5. Dark current of stripe type DSSCs.

electrolyte through porous electrode leads dark current [11,12]. In order to keep the dark current as low as possible direct contact between FTO surface and electrolyte should be minimized. A cell made up of glass frit overcoated Ag grids on both side have low dark current, leading to higher open circuit voltage (V_{oc}). This result shows the full coverage of glass frit layer on Ag grids.

Table 1 shows the photocurrent–voltage parameters of the cells with and without silver current collectors for standard condition (AM 1.5, P_{in} 1000 W/m^2). J_{sc} is almost same for cells

Table 1
I–V parameters of the stripe type DSSCs with and without Ag grids

Cell	Open circuit voltage, V_{oc} [V]	Short circuit current density, J_{sc} [mA/cm^2]	Fill factor [%]	Efficiency [%]
Without grid	0.696	10.0	37.0	2.57
Glass frit overcoat Ag (TiO_2 side only)	0.684	12.71	43.7	3.76
Glass frit overcoat Ag[a] (both sides)	0.716	10.79	60.1	4.64
Laminated Ag grid (both side)	0.676	11.3	63.5	4.85

[a] Spacer thickness 80 μm, others 40 μm, P_{in} 100 mW/cm^2.

with and without current collectors. In one sun condition, fill factor of cell without current collector is very low. This leads to poor efficiency. Overall light to energy conversion efficiency of the glass frit overcoated Ag grid cell is 4.64%. Cells which have surlyn sheet laminated Ag grid also shows similar performance ($\eta = 4.85\%$) in full sun condition.

4. Conclusion

Silver grid lines were prepared on conducting glass substrate by screen printing method. To protect Ag grids from I^-/I_3^- redox electrolyte, crack free 40 μm thick glass frit insulating layer was overcoated on Ag grids by screen printing method. Microstructural images confirm the formation of crack/pinhole free overcoat layer on silver grids. Using these substrates, dye sensitized solar cells were prepared and their *I–V* characteristics studied as a function of light intensity. Overall light to energy conversion efficiency (η) 4.68% was achieved in glass frit overcoated Ag grid cell, which is comparable to surlyn laminated Ag grid cell, its light to energy conversion efficiency was 4.85% under standard condition (air mass 1.5, P_{in} 1000 W/m^2). Now optimizing the dimension of silver grid line and thickness of glass frit overcoat layer for high efficiency are in progress.

References

[1] B. O'Regan, M. Grätzel, Nature 353 (1991) 737.
[2] K. Okada, H. Matsui, T. Kawashima, T. Ezure, N. Tanabe, J. Photochem. Photobiol. A 164 (2004) 193.
[3] G. Phani, M.P.J. Bertoz, J. Hopkins, I.L. Skryabin, G.E. Tulloch, 1997, www.sta.com/download/ewindow-sti.pdf.
[4] M. Grätzel, Prog. Photovolt. Res. Appl. 8 (2000) 171.
[5] G.E. Tulloch, J. Photochem. Photobiol. A: Chem. 164 (2004) 209.
[6] M. Spath, P.M. Sommeling, J.A.M. van Roosmalen, H.J.P. Smit, N.P.G. van der Burg, D.R. Mahieu, N.J. Bakker, J.M. Kroon, Prog. Photovolt. Res. Appl. 11 (2003) 207.
[7] S. Dai, K. Wang, J. Weng, Y. Sui, Y. Huang, S. Xiao, S. Chen, L. Hu, F. Kong, X. Pan, C. Shi, L. Guo, Solar Energy Mater. Solar Cells 85 (2005) 447.
[8] Kurth Glas & Spiegel AG, US Patent no. 6,462,266.
[9] T. Toyoda, et al., J. Photochem. Photobiol. A: Chem. 164 (2004) 203.
[10] H. Matsui, K. Okada, T. Kawashima, T. Ezure, N. Tanabe, R. Kawano, M. Watanabe, J. Photochem. Photobiol. A: Chem. 164 (2004) 129.
[11] M. Grätzel, Pure Appl. Chem. 73 (2001) 459.
[12] K. Zhu, E.A. Schiff, N.G. Park, J. van de Lagemaat, A.J. Frank, Appl. Phys. Lett. 80 (2002) 685.